Title: V-shape Pneumatic Torsional Actuator: A Building Block for Soft Grasper and Manipulator

Authors: Xing Ye, Shidong Zhu, Xiang Qian*, Min Zhang, Xiaohao Wang

*Corresponding author. Email: qian.xiang@sz.tsinghua.edu.cn

Affiliations: Tsinghua Shenzhen International Graduate School, Tsinghua University, Shenzhen, China, 518055

Keywords: torsional actuator, pneumatic actuator, robotic grasper, robotic manipulator

Abstract

Robotic joints are fundamental components in artificial graspers and manipulators, which are designed to achieve high dexterity to carry out various tasks. Traditional robotic hands are often driven by rigid joints, such as tendons and electric motors, resulting in bulky and complex designs. Soft robotics, composed of flexible and compliant materials, offers promising solutions to mimic the human hands and handle delicate objects safely. In this paper, we propose a simple yet effective V-shape pneumatic torsional actuator (V-PTA) as the building blocks of soft grasper and manipulators. The proposed actuator is capable of producing large angular changes and twisting torque, responding fast to pneumatic changes, and scaling to appropriate dimensions easily. Because the design is generic and modular in nature, these lightweight actuators could also be assembled to form a variety of patterns of structures to suit the needs of individual tasks. We further fabricated robotic graspers and manipulators based on multiple V-PTA and demonstrated that our design could offer solutions to execute daily laboratory operations that interact with small and irregular components. Experimental data confirmed that the V-PTA building block structure could potentially pave the path forward for miniature robotic automation in laboratory or industrial settings.

Introduction

From fingers to hands and to wrists, joints are the vital components that make the human hand movable. Despite the structure of each joint varies, it produces one common motion – an angular change between the two connecting skeletal bones. The same is true for robotic graspers and manipulators. Torsional actuators generate twisting motions and apply rotary displacements to drive robotic elements to desired positions.[1] While conventional artificial hands powered by motors have demonstrated promising grasping capabilities,[2, 3] such systems are usually bulky and complicated in nature [4] with reduced robustness as they tend to be susceptible to electromagnetic interference.[5] Rigid motors also limit their abilities to be integrated with flexible components due to structural constraints [6] and lack of safety and adaptability.[7]

In search for better solutions, researchers turned their attentions to alternative operating mechanisms and different actuating materials. Torsional actuators based on carbon nanotube (CNT) yarns,[8-11] polymer fibers,[12-14] shape memory alloys (SMAs) [15, 16] have been proposed with various amounts of actuated torques and angular rotations under a variety of stimuli. Nevertheless, the applications of these torsional actuators are limited by the needs for special actuating environments, including electrolyte,[17] chemical vapor,[9] or heat.[18] There are also substantial challenges to fabricate macroscale devices based on twisted actuators due to difficulties in bulk production of torsional yarns.[1]

Pneumatic artificial actuators have been widely applied in soft robotic fields because fluidic pressures can be easily generated to produce safe and fast actuations as air is widely accessible.[19] Their lightweight structures are beneficial to fabricate soft and flexible robots and therefore offer solutions for new grasper and manipulator designs. While linear pneumatic actuators, exemplified by McKibben artificial muscles,[20, 21] have been extensively studied, their torsional counterparts receive much less attentions. Torsional actuation driven by pneumatic deformation of spiral or helix-shaped tubes were proposed,[22, 23] but their rotary angles are small compared with the lengths of the actuators. Although actuators with pleated chambers could produce significant torque under large positive pneumatic pressures,[24–27] they are prone to bursting due to over pressurization and lead to failure. To circumvent this disadvantage, vacuum-driven actuators are attracting spotlights in recent years. Vacuum (negative pressure)-powered actuators are inherently safe for human-robot interaction as they tend to reduce their sizes rather than expanding during actuation, which effectively eliminate the possibility of bursting. Few such torsional actuators currently exist, including the foam-based actuator [28] and origami-inspired twisting actuator.[29, 30] While both achieved rotary motions under negative air pressures, their actuation trajectories were coupled with reductions in lengths, which may require compensative techniques if pure twisting motions are desired.

Meanwhile, various pneumatic grippers designs have been explored recently. Soft gripper based on pneumatic networks (Pneu-net) [31] can adapt and identify its holding objects aided by proprioceptive sensors.[32] Vacuum-powered finger [33, 34] and magic ball-style grasper [35] can successfully handle a number of soft and delicate objects with great flexibility. Flexible hybrid pneumatic actuators were also applied to a soft humanoid hand with large grasping force.[36] While most of the pneumatic graspers realized versatile holding motions, few have achieved a uniformed torsional structure that combines grasper and manipulator in the same design. We believe it is important to build a control unit that delivers both grasping and manipulating with the same actuation strategy and we seek to address this issue in this work.

Inspired by the fluid-driven origami style muscles,[33] we introduce a simple, easy-to-fabricate, yet effective V-shape pneumatic torsional actuator (V-PTA) design that generates significant angular displacement and twisting torque. Our modular and generic design can achieve reversible and repeatable actuation under vacuum pressure in as fast as 10 ms. Inherently safe and power-efficient, our actuators provide a lightweight

alternative to replace the electric motors commonly used in the robotic field. A single V-PTA structure can work alone as a human-like grasper; furthermore, multiple V-PTAs can be assembled as building blocks to construct different twisting modules and manipulators. The performance of various grasper and manipulators based on this modular design demonstrate that they could produce sophisticated motions to handle various objects commonly found in a chemical laboratory with simple pneumatic control. By introducing this new concept of V-PTA, we help to advance the possibility of deploying lightweight pneumatic robots for laboratory automation.

Materials and Methods

Design concept of the V-PTA

We introduce a vacuum-powered V-PTA design that produces angular displacement and torsional torque when activated. Our actuator features a thin sheet of flexible membrane that encloses two rigid perpendicular plates forming an airtight hollow cavity (Fig. 1A). The thin membrane is made of soft pliable material, preferably non-stretchable, and it is bonded with the plates at contact edges. The relatively rigid plates both act as strain-limiting regions to the thin membrane and also provide structural support to guide the direction of angular deformation. When vacuum is applied to the inner cavity of the structure, it induces tension on the membrane to collapse towards the inside of the assembly and therefore pulls the plates to rotate and fold inward, producing torsional outputs (Fig. 1C; Supplementary Movie S1).

One of the unique features of this design is its generality to produce virtually any rotary motions. One can deploy simple open-loop strategies to accurately control the angles of the actuators by adjusting vacuum pressures. Each actuator is effectively a one degree-of-freedom joint. To produce more complex motions that require multiple degrees of freedom, actuators with different orientations can be assembled to form various combinations to achieve such sophisticated movements. The range of angular changes can also be readily customized. For rotary angles less than 90°, the initial opening angles can be accordingly tailored to suit the needs. Should angles beyond 90° are desired, it is possible to combine multiple V-PTAs in serial to form an actuation group, as we will demonstrate later. The material choices for both plates and membranes are highly versatile as well. Various materials can be used to fabricate the plates provided that they are sufficiently rigid to sustain pneumatic pressures. The membranes should be flexible and easy to be bend. Any thin and inextensible materials that can deform freely are suffice. In addition, the dimensions of the V-PTAs are also configurable to allow easy fabrications under various scales.

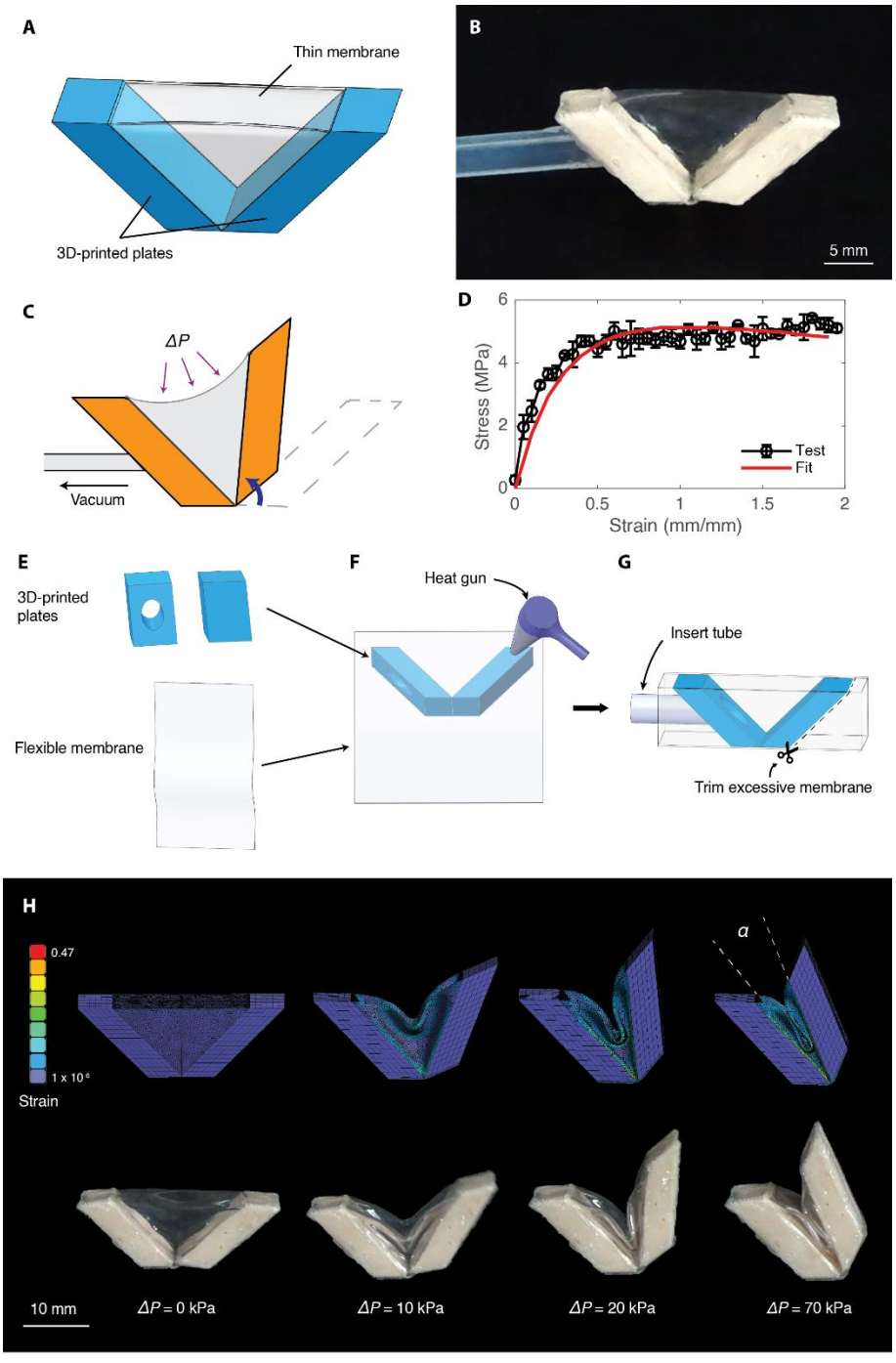
A
Thin membrane
3D-printed plates
B
5 mm
C
ΔP
Vacuum
D
Stress (MPa)
Strain (mm/mm)
Test
Fit
E
3D-printed plates
Flexible membrane
F
Heat gun
G
Insert tube
Trim excessive membrane
H
0.47
1 x 10⁻⁸
Strain
α
10 mm
ΔP = 0 kPa
ΔP = 10 kPa
ΔP = 20 kPa
ΔP = 70 kPa
I
Torsional Angle (°)
Pressure (kPa)
Actuation
Relaxation
Simulation
J
Torque (N·mm)
Pressure (kPa)
Experiment
Simulation

Fig. 1. Design concept and characterization of the V-PTA block. (**A**) The V-PTA block design consists of a thin membrane and 3D-printed plates that forms a sealed structure. (**B**) A prototype of the V-PTA block. The thin membrane of this actuator is a 0.2 mm-thick TPU film. The dimension of the block is 20 mm (length) x 10 mm (width) x 10 mm (height). This actuator weighs 1.70 g (excluding the tube). (**C**) Operating principle of the V-PTA. When vacuum is applied to the actuator, the pneumatic pressure difference induces tensions on the membrane and therefore pulls the plates to rotate. (**D**) The stress-strain curve of the TPU material used in this study was obtained by tensile tests. The results were fitted with the Blatz-Ko hyperelastic model. Error bars show 1 standard deviation (SD) of three samples. (**E**) The simulation results for the actuation processes of the torsional block match experimental data very well. (**F**) and (**G**) show the pressure-torsional angle and pressure-blocked torque relationships of the prototype. Error bars indicate 1 SD of three repeated measurements of a V-PTA.

Actuator fabrication

Because the V-PTA is extremely generic, numerous materials could be utilized to build the actuators using various manufacture methods. Most of the actuators that are covered in this work are composed of rigid plates made of polylactic acid (PLA) and a flexible membrane of thermoplastic polyurethane (TPU) material. The fabrication procedure of a V-PTA starts with building both rigid plates and flexible membranes individually (Fig. 1E). The plates were first virtually constructed in a computer-aided design (CAD) package (SOLIDWORKS Premium 2018, Dassault Systèmes) and then imported to a fused deposition modeling 3D-printer (HORI X500) to fabricate using PLA+ filaments (1.75 mm diameter, eSUN). Two plates were then manually aligned to a perpendicular position. A strip of membrane was cut from a sheet of commercially brought TPU film and placed on top of the PLA-based plates. Since both materials are thermoplastic, a heat gun was used to thermally fuse the contact edges of the plates and membrane to develop high strength connections (Fig. 1F). The temperature of the heat gun was set to 350 – 400 ℃. Excessive membrane materials were then trimmed away after all sides were properly bonded to form an airtight structure. Finally, a silicone tube was inserted through an opening in the plates to the inner cavity for vacuum actuation (Fig. 1G). Different fabrication procedures may be required if other materials were used to construct the actuators. For actuators whose membranes are cut from silicone or Polyethylene (PE) sheets, one can could simply glue the membranes to the plates to form the sealed structures.

Finite element modeling

We first characterize the mechanical properties of the TPU membrane in order to simulate its performance in the numerical models. The stress-strain relationship of the TPU film was obtained in a uniaxial tensile test on an electric static testing instrument (ElectroPlus E3000, Instron). Three samples of the membrane were prepared by cutting a 0.1 mm thick TPU film to a dimension of 15 mm (length) x 5 mm (width). All samples

were pulled at a constant speed of 3 mm/min to approximately 200 % strain change. The results were then fitted with the Blatz-Ko hyperelastic model (Fig. 1D).

We developed two numerical static analysis models to simulate both free-load actuations and blocked-torque measurements in Ansys Mechanical (2019 R1). Only a quarter of the full model were built to take advantage of the two symmetric planes. The plate of the actuators was meshed with hexahedrons and the film was meshed with tetrahedrons. A bonded connection was set up between the plate and the membrane. Frictional contact pairs were also defined for the inner and outer surfaces of the membrane to simulate the folding deformation and prevent self-penetration. All faces on the symmetric planes were frictionlessly supported. The air pressure was directly applied to the inner surface of the model to mimic the vacuum application. For the free-load simulation, the end point of the plate was traced by a pair of deformation probes. For the blocked-torque simulation, a force reaction probe was set up to determine the force at a direction normal to the plate.

Results

V-PTA Characterization

We fabricated a prototype of the V-PTA using thermoplastic polyurethane (TPU) film and three-dimensional (3D)-printed polylactic acid (PLA) plates (Fig. 1B). A vacuum pump of 300 L/min air displacement was supplied as the pressure source in this study. The air pressure inside the actuators was controlled by an electronic vacuum regulator (ITV2090-21N2BL5, SMC). The control signal for the vacuum regulator was generated by a microcontroller (Arduino Mega 2560) via a I2C-based digital-to-analog convertor (DAC) microchip board (MCP4725, Adafruit).

The actuator was secured on a test stand and was loaded with different vacuum pressure while the torsional angle changes $\Delta\alpha$ under no load and the blocked torque τ were recorded (Fig. 1, I and J). For the torsional angle measurements, the vacuum pressure was set up to increase linearly up to 60 kPa at a speed of 1 kPa/s. A camera was used to record the displacement of the free end at 20 – 30 frames per second. The recording was then examined in a video analysis tool (Tracker) to obtain torsional angles at each air pressure. For the blocked torque measurements, an additional force gauge (RZ-1, Aikoh Engineering) was mounted on a motorized linear translation stage. The force gauge was positioned so that the tip of the gauge was just touching the free end of the actuators. Step inputs of vacuum pressure were applied to the actuators and the maximum forces registered by the force gauge were recorded.

The actuator was extremely sensitive to small pressure difference as it produced 70 % of the maximum torsional angular stroke at 10 kPa vacuum pressure. The maximum angular contraction ratio was approximately 80 % as the membrane folds inward during actuation that unavoidably affects its ability to fully reach its designed angle. We also observed very low hysteresis between the actuation and relaxation processes, which is favorable

for reversible actuations. The specific torque (*i.e.*, normalized to actuator mass, 1.70 g) of this prototype at 70 kPa pressure was 26.6 N·mm/g, which greatly exceeds that of commercial electric motors (2 – 6 N·mm/g).[9] The pressure-torque curve exhibits non-linear relationship. This behavior is more obvious when vacuum pressure is high as the film starts to fold and adhere to the side walls of the plates and therefore produces pushing forces adverse to the torque output direction.

Fig. 1, H-J and Supplementary Movie S2 compare the experimental data with simulation results. The numerical models accurately predicted the trends of both pressure-torsional angle and pressure-torque relationships, yet the simulation results overestimated the torque output by up to 26.4 %. This variation may due to mismatch between the pulling speed during tensile tests and the actual actuation speed or minor plastic deformation of the TPU film during repeated actuations.

Parametrical optimization

Because the V-PTAs are of generic design, a variety of parameters could be customized to suit the needs of individual tasks. We first investigate the effects of materials of the thin film on the performance of these actuators. The mechanical properties of three off-the-shelf membranes (Polyethylene (PE), TPU, and silicone) were obtained by uniaxial tensile tests and their elastic moduli were approximated by the slopes of the linear regions in their corresponding stress-strain curves (Fig. 2A). V-PTAs of the same dimension but with different film materials of the same thickness (0.1 mm) were characterized by their performance (Fig. 2, B and C). For the softest material (silicone), the experimental results suggested that while the actuator was easy to deform and achieved a large angular change under very low vacuum pressures (produced 70 % of maximum torsional stroke at 8 kPa), the film quickly buckled under high pressures and yielded the lowest torque output. A stiffer material (PE) could benefit from producing larger torque output, yet the angular stroke suffered from its inflexibility. A delicate balance must then be chosen to produce enough torque while maintaining favorable angular contraction ratio. We further fabricated actuators of the same material (TPU) but with different film's thickness (Fig. 2, D and E). A similar conclusion could be drawn that while a suitable thickness of film was required to properly transmit torque output, it should also not hinder the bending deformation to achieve proper angular stroke.

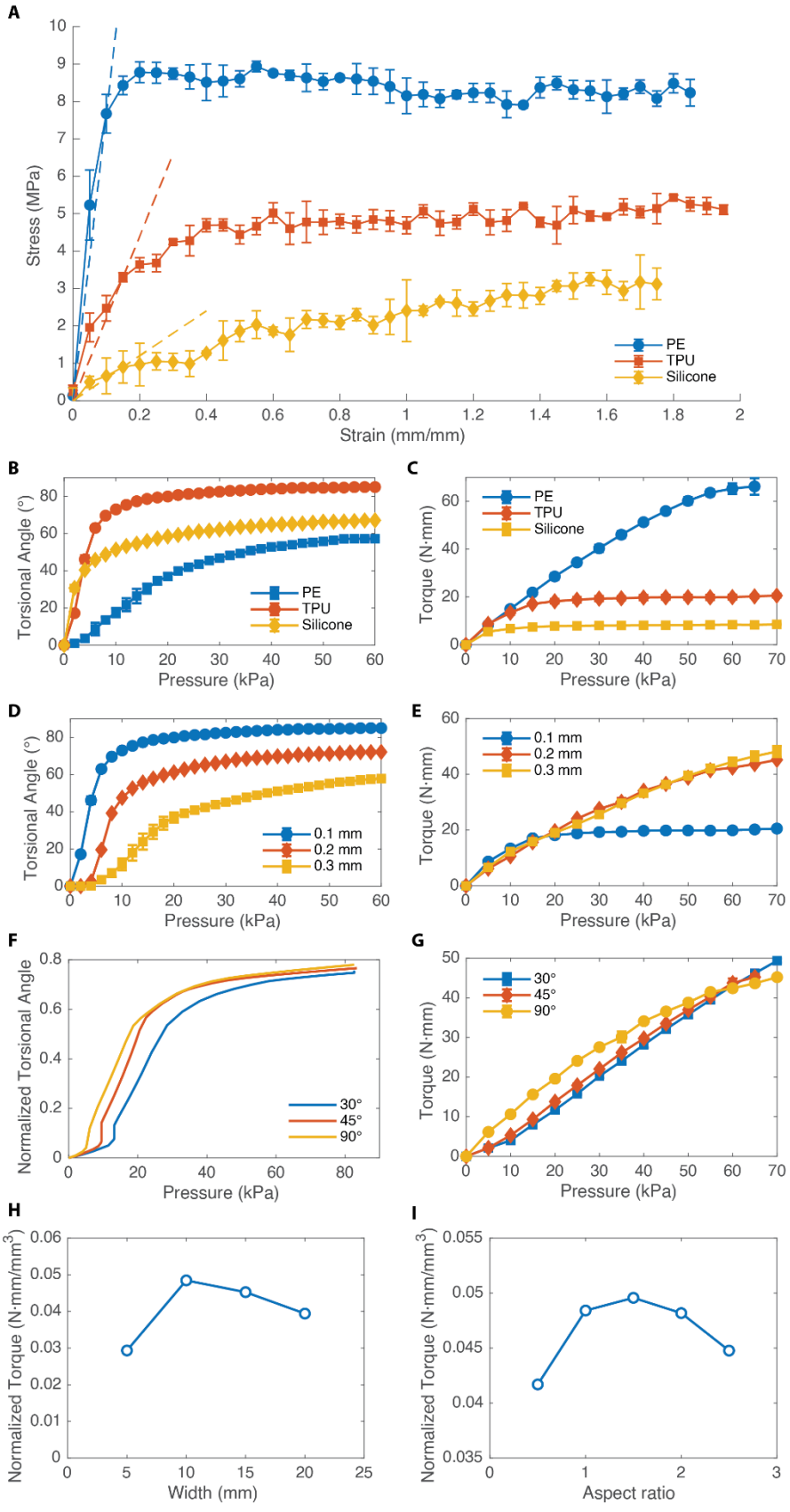
A
Stress (MPa)
Strain (mm/mm)
PE
TPU
Silicone
B
Torsional Angle (°)
Pressure (kPa)
PE
TPU
Silicone
C
Torque (N·mm)
Pressure (kPa)
PE
TPU
Silicone
D
Torsional Angle (°)
Pressure (kPa)
0.1 mm
0.2 mm
0.3 mm
E
Torque (N·mm)
Pressure (kPa)
0.1 mm
0.2 mm
0.3 mm
F
Normalized Torsional Angle
Pressure (kPa)
30°
45°
90°
G
Torque (N·mm)
Pressure (kPa)
30°
45°
90°
H
Normalized Torque (N·mm/mm3)
Width (mm)
I
Normalized Torque (N·mm/mm3)
Aspect ratio

Fig. 2. Parametrical study of the V-PTA block. (**A**) The stress-strain relationships of three commercially-available membranes were obtained by uniaxial tensile tests and the linear regions were fitted with dash lines to approximate their elastic moduli. Each test was repeated for three samples of the same material. (**B**) and (**C**) present the actuation results of V-PTAs with different membrane materials of the same thickness (0.1 mm). (**D**) and (**E**) show the characterization of V-PTAs with TPU films of different thickness. (**F**) plots the simulation data of actuators with different opening angles. The results were normalized against their respective initial angles. (**G**) demonstrates the blocked torques of three V-PTAs with interconnected chambers of various opening angles. All measurements were repeated three times for a V-PTA and SDs are indicated by error bars.

We next explored the effect of initial opening angles of the actuators on angular changes using simulation models. The torsional angular stokes of three actuators with opening angles of 90°, 45°, and 30° were analyzed by normalizing torsional changes against their designed angles (Fig. 2F). The simulation results revealed that while large initial angles translated to higher normalized angular stroke, likely due to less interference between different segments of the film during bending deformation, the opening angles had no significant impact on the final contraction ratio. In light of these results, we assembled three actuators consist of interconnected chambers of various opening angles to study if the initial angles could affect their torque measurements (Fig. 2G). The blocked torque results also suggested that opening angles mattered little in actuators' performances. This gives us the maximum flexibility to design torsional actuators with appropriate configurations of opening angles without concerning about potential impacts on their performances.

We also address the need to customize the dimension of the actuators to conform various sizes of objects in the real world. Our actuators can be easily scaled to various dimensions by changing the widths, lengths, and heights. To simplify the comparative studies, we kept the ratio of the length of actuators to their height as 2:1 to ensure that the opening angles were fixed at 90°. The blocked torques of a variety of actuators with different dimensions were studied using finite element modeling techniques. We introduce an aspect ratio λ to represent relative dimension of the height to the width of a torsional actuator. We first kept the aspect ratio λ to 1 and compared torsional actuators at multiple scales whose widths ranged from 5 mm to 20 mm. The normalized blocked torques (relative to the volume encased by the film) of actuators at vacuum pressure of 40 kPa were obtained through numeric analyses (Fig. 2H). On the basis of the computational prediction results, actuators with width of 10 mm produces larger relative blocked torque than actuators with other dimensions. Keeping the widths at 10 mm, we varied aspect ratios λ from 0.5 to 2.5 by adjusting the heights of actuators from 5 mm to 25 mm. The results suggested that actuators with ratios 1 – 1.5 yielded larger normalized torques (Fig. 2I). These simulation data advise that the width and heights should generally be kept at similar dimensions to produce greater torque output.

Dynamic performance

We characterized the step response of a V-PTA with 0.1 mm-thick TPU film. A 6 V-powered three-channel solenoid valve (ZHV-0519) was used to switch between vacuum pressure and atmospheric pressure. The valve was triggered by a square wave generated from a digital pin of Arduino Mega 2560 with a period of 2,000 ms and a duty cycle of 50 %. Both positive and negative step responses could be examined in this setup.

The vacuum pressure was first switched on for 1000 ms and then switched off while a high-speed camera was recording the angular deformation process of the actuator at 5000 frames per second. The sequential images were then analyzed in Tracker to extract angular strokes. The vacuum pressure inside the actuators was also simultaneously measured by a pressure sensor (GZP040S) and recorded by a data acquisition device (USB-6009, National Instruments) at a sample rate of 1000 Hz. The pressure sensor was calibrated with a microfluidic flow control system (MFCS-EZ, Fluigent) in advance and the slope of the calibrated voltage-pressure relationship was used to map the output voltage of the sensor to the vacuum pressure within the actuators.

The results revealed that the actuator quickly achieved the maximum torsional angles in 31 ms since the step control signal started, even as the vacuum pressure inside the actuators was still rising and merely registered as 11 kPa at the instant (Fig. 3A). The rise time of the step response, defined as the elapsed time between 10 % and 90 % of the maximum angular stroke, was 10 ms, while the fall time was 22 ms. The rapid responses to pneumatic pressure changes are highly advantageous in high frequency applications. Nevertheless, the actuator also experienced oscillations and it took 58 ms to settle within ± 2 % of the final steady-state angle. We note that the underdamped nature of the step response would be challenging to accurately control the angles of the actuators and bistable control strategy may be preferred in that case. A 9 ms delay between the onset of rising vacuum pressure and the start of control signal was likely introduced by the switching speed constraint of the solenoid valve.

Next, we investigated the maximum actuation frequency that the V-PTA could act. A series of square waves of 10 Hz and 20 Hz frequencies were generated to control a solenoid valve and the torsional angular displacements were simultaneously recorded. Fig. 3B showed the angular changes of the actuator as time progressed. The response curves followed the same periodic patterns of the control signals. The peaks of angular strokes did not achieve the maximum torsional angles of static responses, not did the valleys of displacements dropped to 0, likely because the actuator did not have enough time to fully inflate and deflate. We inferred from the results that the actuation frequency could be further increased at the expense of reduced angular amplitude. However, due to performance limitation of the solenoid valve, and also such high frequency dynamic performance is trivial in artificial grasp applications, we did not perform tests with stimulating waves of frequencies higher than 20 Hz.

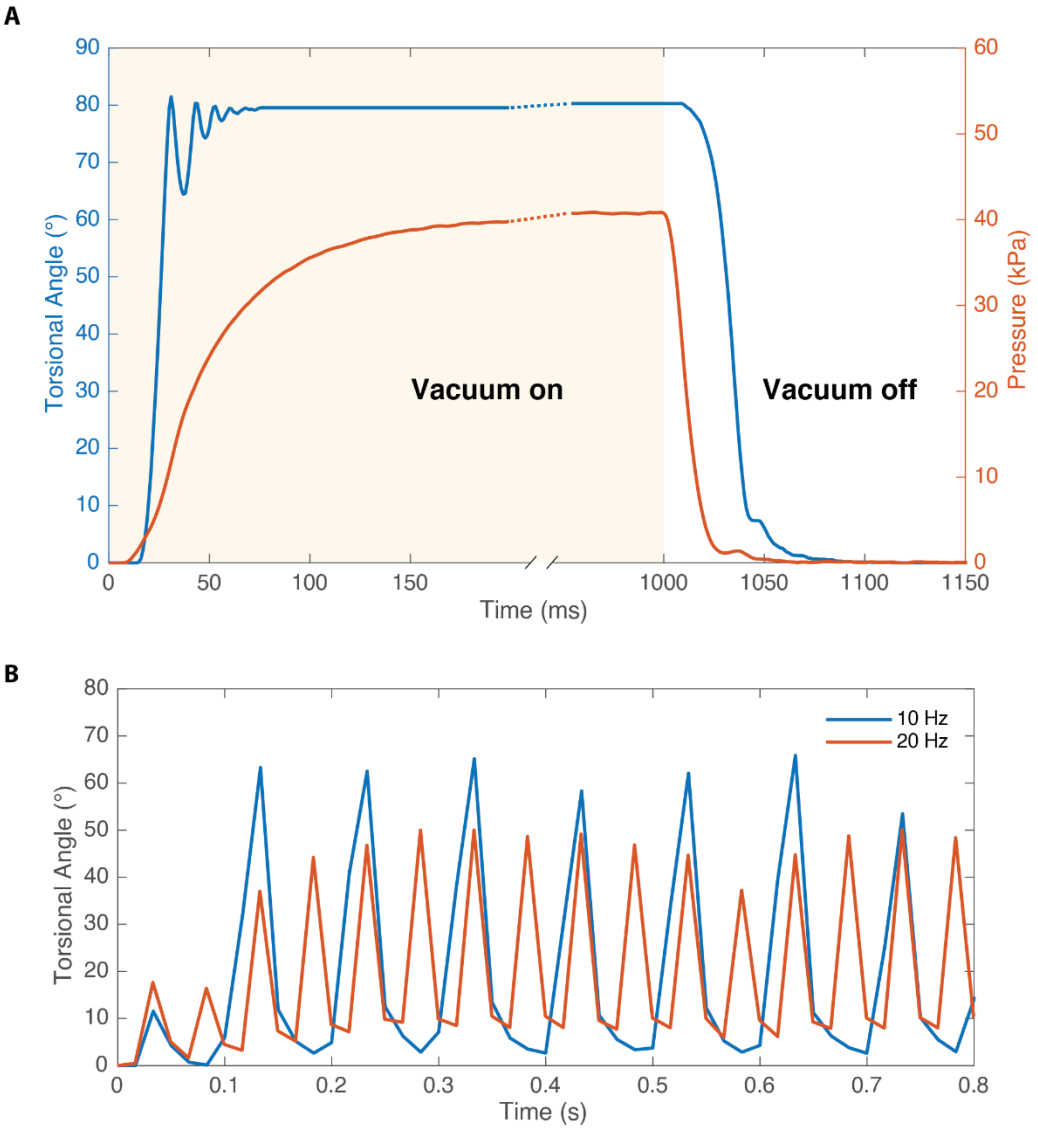

Fig. 3. Dynamic performance of the V-PTA block. (**A**) A V-PTA with 0.1 mm thick TPU membrane was actuated for 1000 ms and then deactivated. The torsional angle changes and vacuum pressure inside the actuator were recorded. (**B**) A V-PTA with 0.2 mm thick TPU was actuated by square waves of control signals with different frequencies. The torsional angle data suggest that the actuator responded fast to pneumatic pressure changes.

Comparison with other torsional actuators

Our V-PTA produces angular changes during actuation, similar to the behavior of a servomotor. We compare our vacuum-powered torsion actuator with a commercially available electric micro servomotor (SG90, Tower Pro) (Fig. 4, A and B). Even though the pneumatic actuator is lighter (2.73 g versus 9 g) and occupies less volume (5.6 cm^3 versus 8.1 cm^3) than the electric counterpart, both devices successfully lifted a load of

100 g repeatedly (Supplementary Movie S3). This demonstration suggested that our torsional actuator design could effectively provide drop-in replacement of servomotors commonly used in miniature robotic field. However, we noticed a slight deformation of the thin film before contraction due to pretension applied to the actuators by the loads. This behavior could potentially be detrimental to effective actuations and could be mitigated by choosing appropriate materials and thickness of the film to match anticipated carrying loads.

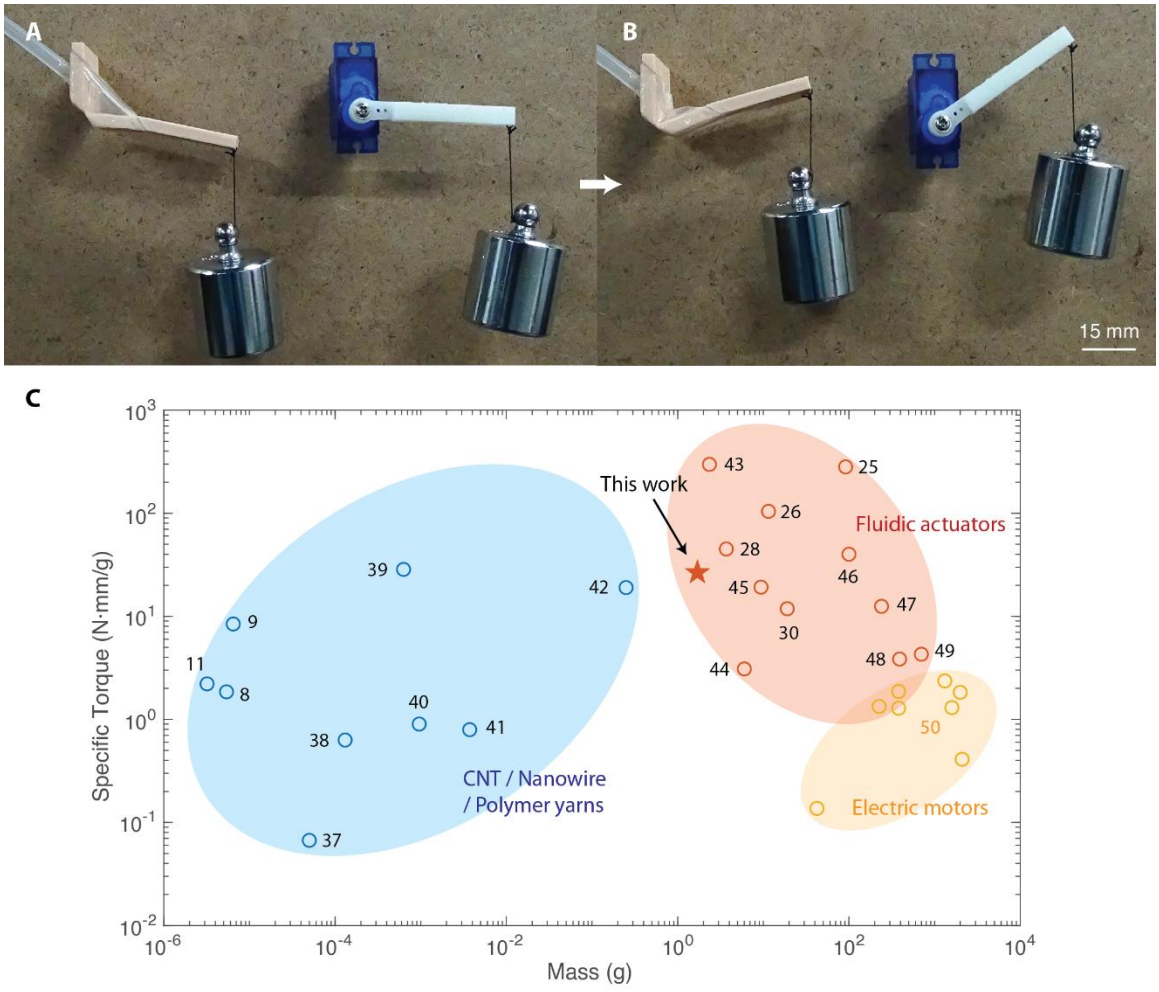

Fig. 4. Comparison between V-PTA design and other torsional actuators. (**A**) and (**B**) showed that both a V-PTA and a servomotor successfully lifted weights of 100 g. Our vacuum-powered actuators could provide drop-in replacements of servomotors. (**C**) lists masses and specific torques of various artificial torsional actuators with different operating principles. Torsional actuators based on yarns and fibers are currently not practicable to build macroscopic devices. Our actuator design is lightweight compared with other fluidic actuators and still provides torques exceed those of electric motors. The annotation number of each data point refers to corresponding citation index.

Fig. 4C lists the masses and specific torques of some artificial torsional actuators with a variety of materials and operating principles. Torsional carbon nanotube (CNT) actuators and polymer yarn based artificial muscles generate large and high-speed angular rotations in the presence of various stimuli, but it remains challenging to fabricate macroscopic appliances. Electric motors prove to be powerful actuation devices for robotic applications, yet their specific torques are currently limited and the inherent heavy weights restricted their applications in soft robotics field. Pneumatic torsional actuators bridge this gap by achieving large torque output and maintaining suitable sizes to mimic the human muscles. Our pneumatic actuator design strives to balance between maintaining an airy weight and producing relatively large twisting angles. Compared with other types of torsional actuators, this design features a lightweight, extremely fast and powerful solution to produce angular rotation in soft robotics. Meanwhile, the torsional angular strokes of the actuators normalized to their heights are within 7 – 9 °/mm, which are the highest results among fluidic torsional muscles reported in literature.[22, 29] It further proves that the V-PTAs are unique in being safe, fast and strong components to provide powerful torsional actuations.

Single V-PTA works as a robotic grasper

To demonstrate the potential applications of our V-PTA in robotic systems, we built a grasper based on a single torsional actuator that serves as a one degree-of-freedom joint to mimic the pinching movement of the thumb and index finger of a human hand (Fig. 5, A and B). The grasper is capable of holding objects by applying adequate normal forces to prevent them from slipping, just like how the human hands pick up small objects. A thin layer of Ecoflex (00-35, Smooth-On) was brushed and cured on the tip of the grasper to further increase frictional contacts.

We first investigated the holding forces exerted by the grasper using a flexible force sensor (FlexiForce A201, Tekscan). The low force range (0 – 4.4 N) of the sensor was suitable for our grasping application. The sensor was fed with 5.0 V power input (Keithley 2280S-60-3 DC power supply, Tektronix) and the amplified voltage output was read by a digital multimeter. The RZ-1 force gauge, mounted on a motorized stage, was used to calibrate the sensor. The force sensor was secured on a flat surface for ease of force applications. Activation forces of 4.0 – 5.0 N were applied to the sensor for five times in advance. Forces range from 0 – 2.10 N were subsequently applied to the sensor and the corresponding voltage outputs were recorded.

The force sensor was put between the arms of the grasper to record its contact forces. Both actuation forces without holding objects and blocked forces were measured against different vacuum pressures. For the actuation forces measurements, the force sensor was directly held by the grasper. For the blocked forces measurements, an object with the same length of the distance between the arms of the grasper in unactuated state was held by the grasper to fix its movement and the contact forces required to hold the object was

recorded. The voltage outputs of the sensor were mapped to their corresponding forces using linear interpolation and extrapolation of the calibration data at desired points. The results revealed that the grasper was able to deliver gripping forces up to 1.40 N and blocked forces up to 1.57 N at 70 kPa pressure (Fig. 5C). The actuation forces were slightly less than the maximum blocked force due to further buckling of the thin film as the joint angle changed to allow the tips of the graspers come into contact.

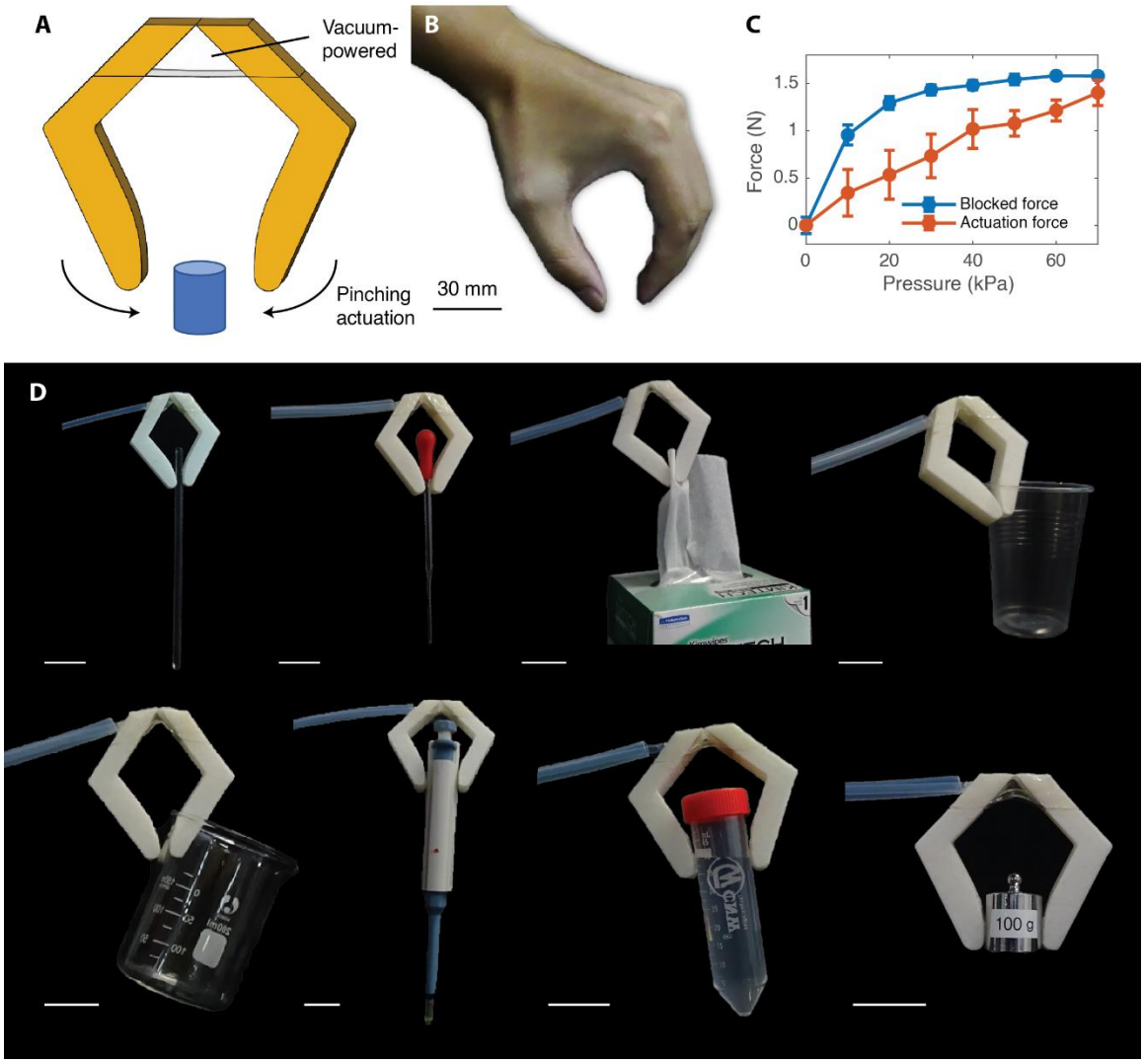

Fig. 5. A grasper powered by a single V-PTA. (**A**) The grasper delivers pinching motions upon vacuum application. (**B**) The grasper design is inspired by the pinching movement produced by the thumb and index finger of a human hand. (**C**) Both actuation forces without holding objects and blocked forces of the grasper were measured by a force sensor. Error bars show 1 SD of three tests. (**D**) The grasper is capable of holding various objects found in a laboratory. The V-PTA-based grasper can hold a glass rod, a glass pipette, a piece of cleaning wipe, a plastic cup, a glass

beaker, a mechanical pipette, a centrifuge tube contained with liquid, and a calibration weight of 100 g. Scale bars represent 30 mm.

We next verified whether the level of force output of the grasper is adequate to hold several objects. A variety of appliances commonly found in a laboratory were used to test the grasping capability of our grasper. We deployed an open-loop control strategy where a fixed vacuum pressure (70 kPa) was used to actuate the grasper in all tests. The pneumatic grasper successfully held objects both light (glass rod, cleaning wipe, and plastic cup) and heavy (glass beaker, mechanical pipette, and calibration weight) (Fig. 5D; Supplementary Movie S4). These items possess diverse masses range from 2.40 g (plastic cup) to 100 g (calibration weight) and gripping thicknesses range from 0.05 mm (cleaning wipe) to 28.37 mm (centrifuge tube). It shows that our grasper is extremely compliant and versatile to adapt to various shapes and weights of the holding objects without complex pneumatic control systems. The performance validated that the grasper could be used to manipulate various equipment in laboratory settings.

Assembling multiple V-PTAs

While single V-PTA is designed to deliver angular strokes less than 90°, more complicated motions can be achieved by combining multiple actuators in various configurations to form different actuator modules.

One of the advantages of using elastic materials in actuator design, such as TPU films in this study, is that the actuators can inherently possess the ability to achieve reversible actuation. When the torsional actuators are bending during application of external vacuum pressure, they also store elastic energy to return their original shapes once vacuum is withdrawn. Fig. 6A shows the blocked torques of both actuation and relaxation processes of a torsional actuator. While the relaxation torque paled in comparison with the actuation torque (less than a quarter of that of actuation process), it still provides enough force to rapidly restore itself when vacuum is disconnected.

Applications may arise that equally large torques are desired to achieve bidirectional actuations. Two antagonistic actuators, each with individual pneumatic line, can be bonded to form a bidirectional module. Only one of the two actuators is pressurized at any time while the other side is open to atmospheric pressure. The actuation direction is controlled by which side the vacuum is connected to. Fig. 6B and Supplementary Movie S5 demonstrates the scheme for this configuration and the blocked torques measurements. The results effectively combine both actuation and relaxation torques to produce even larger torsional output at both directions since the antagonist pair is undergoing different processes at each side. While this arrangement appears to be more complex than a single actuator, it nevertheless proves its usefulness when symmetric bidirectional torque performance is desired.

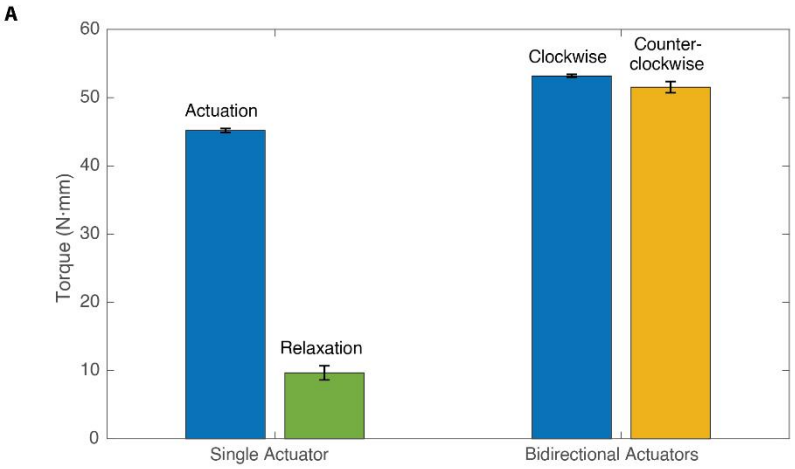
A
60
50
40
30
20
10
0
Torque (N·mm)
Actuation
Relaxation
Clockwise
Counter-
clockwise
Single Actuator
Bidirectional Actuators

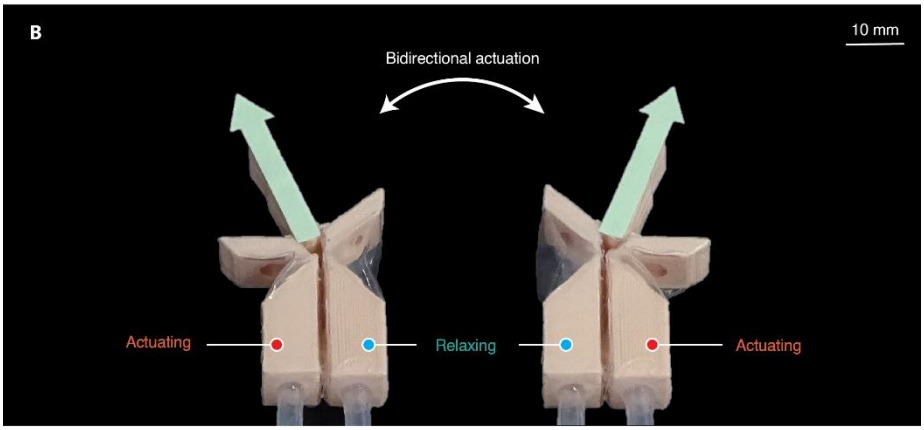
B
10 mm
Bidirectional actuation
Actuating
Relaxing
Actuating

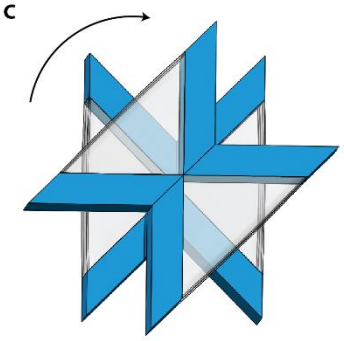
C

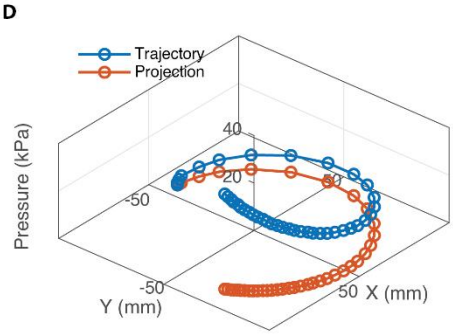
D
Trajectory
Projection
Pressure (kPa)
40
20
0
-50
-50
Y (mm)
50
X (mm)

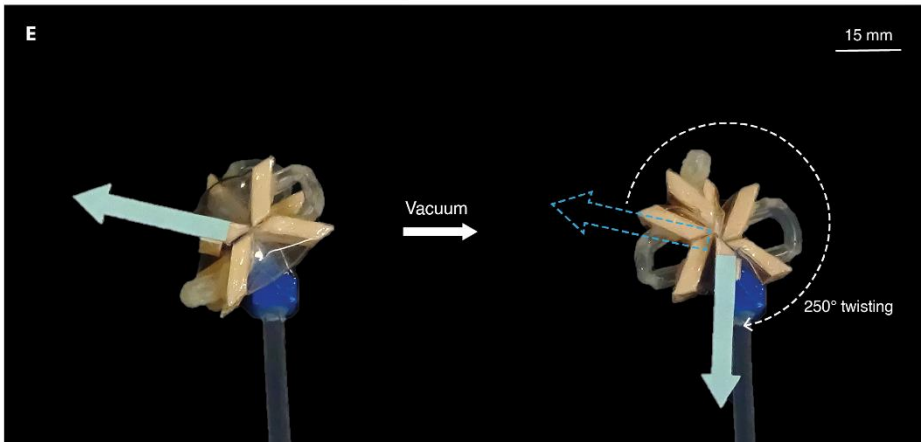
E
15 mm
Vacuum
250° twisting

Fig. 6. Multiple V-PTAs can be assembled to produce complex motions. (**A**) Comparison between the blocked torques of a single actuator and a bidirectional actuator module confirms that the combined module could produce larger and symmetric torques in both directions. (**B**) The actuation principle of the bidirectional module. Only one side of the individual actuator is activated while the other side is relaxing. (**C**) Four actuators connected in series form a super-twisting module. (**D**) The position of an end point on the twisting module was plotted against different vacuum pressures. (**E**) The actuation process of a super-twisting module shows that it could produce up to 250° angular changes.

For applications that require large angular displacement beyond 90°, we demonstrate that it is also possible to increase the actuated torsional angles by simply combine multiple V-PTAs in serial. Fig. 6C presents such a super-twisting module that employs four actuators to boost the actuation angles up to four folds. Each actuator is inter-connected to others with external tubing to allow simultaneous actuations with a single pneumatic control. Upon vacuum application, all actuators rotate in the same direction to deliver a twisting motion. Care should be taken to align the torsion axis of each actuator during fabrication to prevent imbalanced motions. A wrist structure fabricated based on this technique achieved angular changes up to 250° (Fig. 6, D and E; Supplementary Movie S6), which is higher than previous reported results [22, 29] and acts as a transhuman-like wrist.

V-PTAs-based manipulator handles a centrifuge tube

Many appliances employ screwing mechanism to allow easy opening and closing. Centrifuge tube is one of the common utensils in a laboratory that requires a series of twisting motions to open its cap. For robotics systems, this presents a great challenge since large torsional angles are necessary to automate this process.

To illustrate possible applications in automation of laboratory procedures, we built two manipulators based on several V-PTAs building blocks to demonstrate robotic bimanual operations. One manipulator was for mimicking the right hand to grasp centrifuge tube with one finger, similar to the structure presented by Li et al.,[33] and dump the liquid through rotating its wrist using the bidirectional module design as mentioned above (Fig. 7A). The other manipulator was for mimicking the left hand to grasp the cap of the tube with one finger and unscrew the cap through rotating a transhuman-like wrist with a super-twisting module also mentioned above. The soft robotic manipulators cooperated to perform the experiment successfully, as shown in Fig. 7B and Supplementary Movie S7.

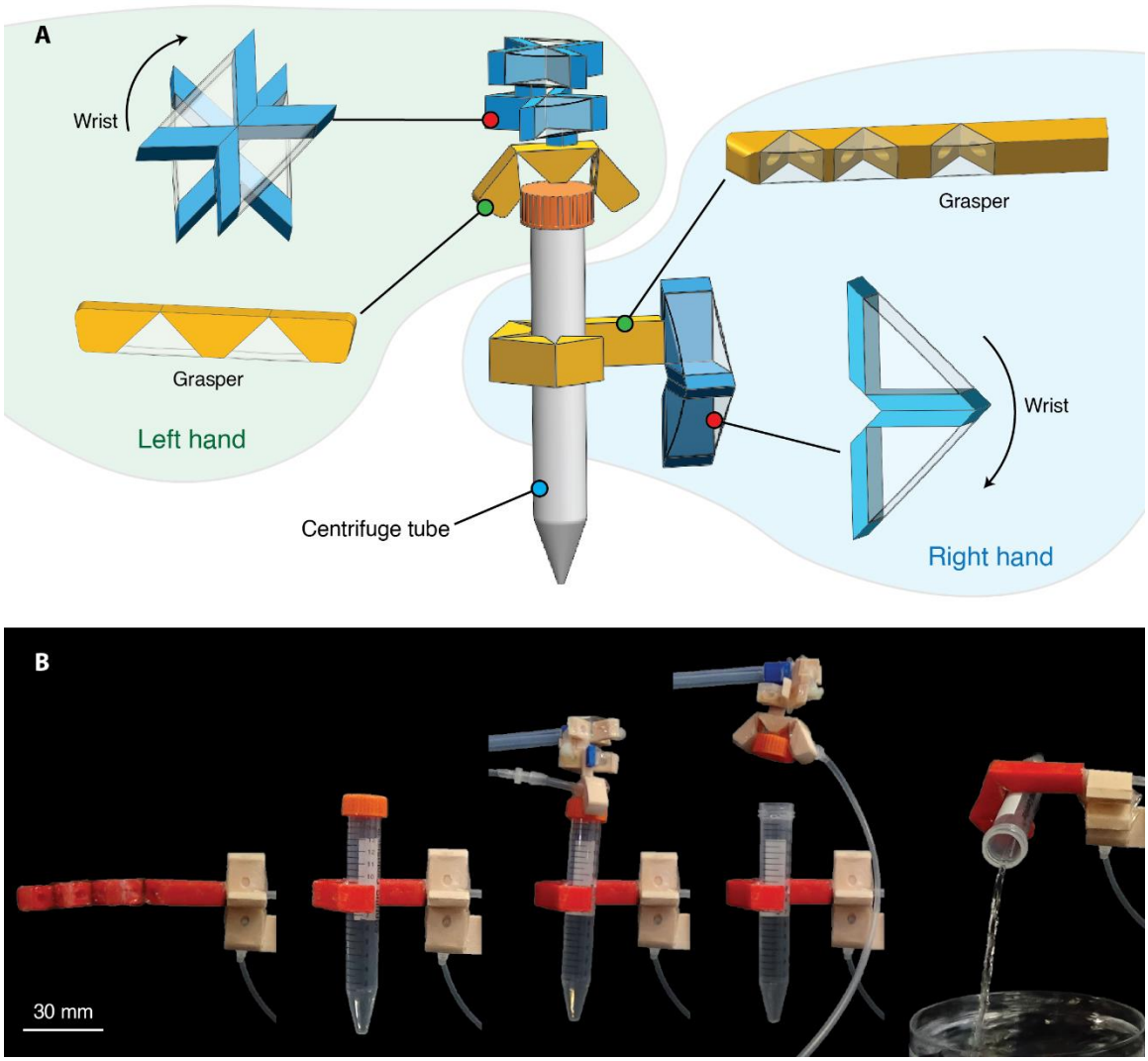

Fig. 7. Bimanual cooperation of V-PTAs-based manipulators that handle a centrifuge tube. (**A**) Both the left hand and right hand are mimicked using V-PTA as building blocks. The left hand is charged with holding the cap of a centrifuge tube and unscrewing it. The right hand is tasked with holding the centrifuge tube and pouring off the liquid. (**B**) The manipulators successfully grasp a centrifuge tube, screw off its cap, and dumping the liquid inside of the tube.

V-PTAs-manipulator handles a plastic pipette

Liquid transfer is a fundamental procedure in countless lab operations. While human hands are dexterous enough to operate pipettes, it is difficult for soft robots to apply suitable forces to the bulb of a pipette to manage the liquid inside while accurately control its position.

We built a soft manipulator based on V-PTA building blocks to demonstrate its flexibility to handle a plastic pipette. The manipulator consists of three modules which are independently controlled by either a solenoid valve or an electronic vacuum regulator

(Fig. 8A). The linear module is made of two V-PTAs connected in serial whose torsional actuation direction are opposite. During vacuum actuation, both actuators contract and their torsional effects are cancelled out to achieve a linear motion. The linear module is useful to control the vertical movement of the pipette to either submerge it into liquid or lift the pipette out of liquid. The tilting module is a single V-PTA used to control the direction of the pipette. At relaxed state, the end point of the actuator tilts to the right side. With proper vacuum pressure, it can move to the neutral or the left side. This module is used to tilt the pipette to point to desired locations. The grasping module is just a single V-PTA based pinching fingers as described above to hold the pipette, yet with a modification that two modes of vacuum pressures can be applied to the actuator to achieve different grasping behaviors. A lower pneumatic pressure (10 kPa) allows the grasper to deliver adequate forces to securely hold the pipette but do not squeeze its bulb. The higher vacuum pressure (70 kPa) enables the grasper to pinch on the bulb of the pipette to empty it of air or dispense the liquid inside (Fig. 8C).

To determine the repeatability of the liquid drawing process, we programmed the manipulator to suck up water and then dispense the liquid it held into a Petri dish where the water can then be weighted. This process was repeated ten times and the volumes of the drawn liquid are shown in Fig. 8B. The manipulator drew up an average of 0.609 mL liquid into the pipette with 2 mL capacity. The repeatability measure of ± 0.016 mL accuracy shows that the manipulator could exert relatively constant forces on the pipette to achieve a reliable fluid flow.

We next used the manipulator to control a plastic pipette and conduct a chemical experiment involving mixing copper sulfate ($CuSO_4$) and sodium hydroxide (NaOH) solutions to demonstrate the potential of laboratory automations (Fig. 8D; Supplementary Movie S8). Both solutions contained 2 weight percentage of their respective solutes and were dispensed in Petri dishes in advance. The pipette first drew up a small quantity of NaOH (colorless) solution and then introduced it into the $CuSO_4$ (blue) solution. A pale blue gelatinous precipitate of copper hydroxide ($Cu(OH)_2$) was formed in the mixture. Next, the pipette stirred the solution to speed up the chemical reaction by repeatedly actuating the tilting module back and forth. Finally, a small portion of $CuSO_4$ solution was added to the NaOH solution to demonstrate reversible actuation. Our manipulator was highly versatile in handling the pipette and successfully completed all steps required in this chemical experiment.

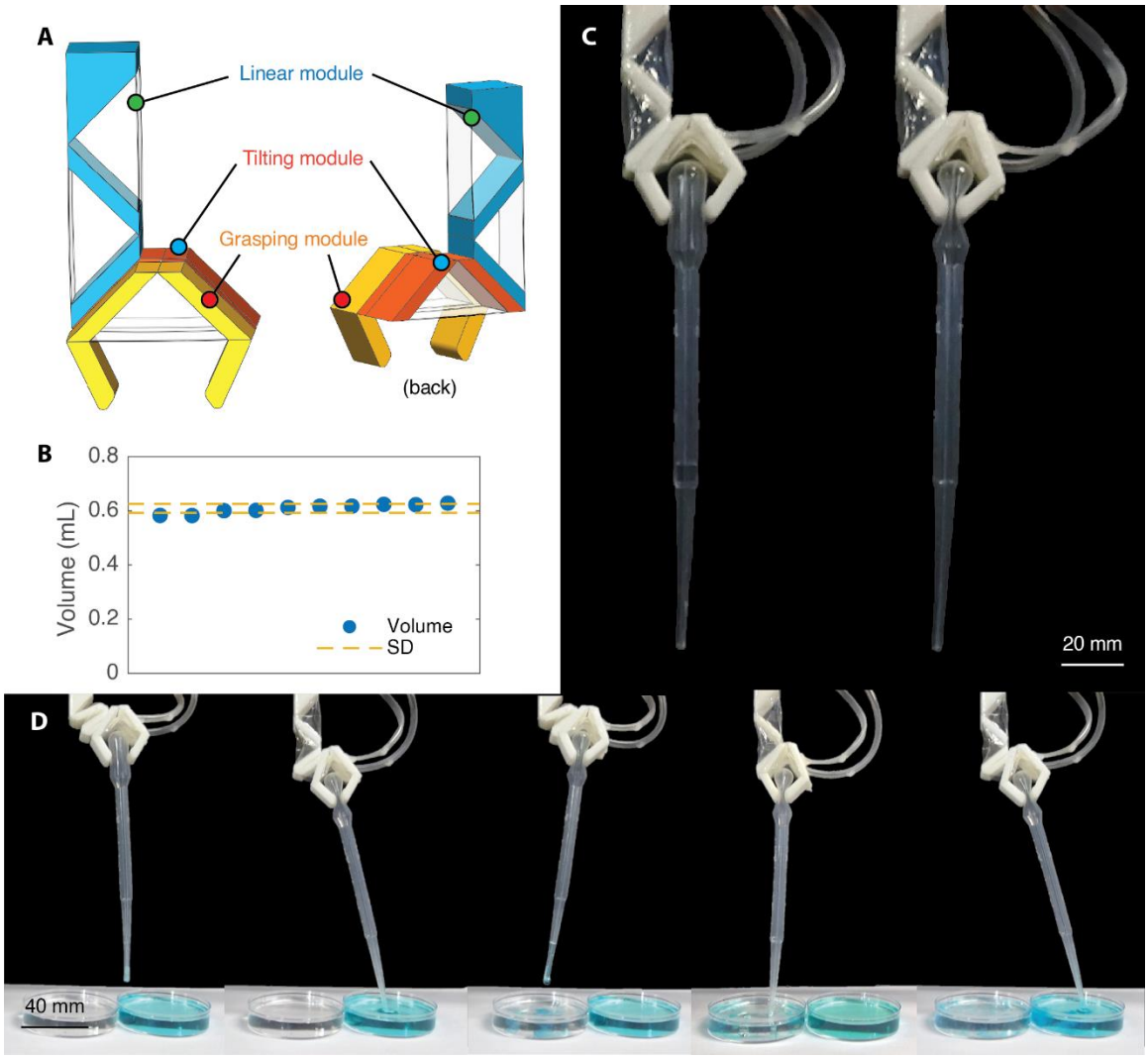

Fig. 8. V-PTAs-based manipulator handles a plastic pipette. (**A**) The manipulator consists of a linear module, a tilting module, and a grasping module. (**B**) The manipulator drew up steady amounts of liquid into the pipette. Dash lines represent 1 SD of ten tests. (**C**) The grasper exerts different holding forces on the pipette to either hold it but do not squeeze its bulb or pinch on the bulb to dispense the liquid. (**D**) The manipulator successfully conducted a chemical experiment involving mixing copper sulfate ($CuSO_4$) and sodium hydroxide (NaOH) solutions.

Conclusion

Here, we presented a vacuum-powered V-PTA design that features powerful, fast, safe, and repeatable actuations. Our flexible actuators can be easily manufactured at various scales using common inexpensive materials. Experimental and simulation data confirmed that the actuators could produce large twisting torque and significant angular changes in short duration of time. Multiple V-PTAs could be assembled to achieve special motions, including bidirectional and super-twisting actuations. Furthermore, we constructed a series of miniature robotic graspers and manipulators to demonstrate their performances

in handling various objects and executing basic operation in daily lab working using the V-PTAs as building blocks. Our results illustrated that these lightweight, modular and generic structures are strong candidates for building small-scale robotic manipulators that require rotary motions. Complex movements that mimic the functions of a human hand can also be realized by combining individually-controlled assembled modules. Thus, our V-PTA design offers new solutions for driving delicate manipulators and could pave the path forward for miniature robotic automation in laboratory or industrial settings.

The simplicity of our pneumatic actuator design does not preclude its potential to be further expanded to include additional features. While open-loop control strategy with preset pneumatic pressures achieved excellent performances in our demonstrations, it is possible to integrate feedback sensors to deliver predictable and accurate trajectories. For example, flexible pressure sensors could be applied at the tip of the pneumatic grasper to monitor and adjust the holding forces to adapt to different holding objects. Additional inertial measurement units (IMU) that combine accelerometers and gyroscopes can also be included to further calibrate the angular motions of the torsional actuators. Our manipulator can also be assisted by machine vision algorithms to recognize and locate the positions of items for full adaptability in laboratory automation applications. These ideas will be further explored in our future works.

Acknowledgments

We thank Jiaming Liang in Tsinghua-Berkeley Shenzhen Institute for assistance with high-speed camera recording and Yushi Li in Tsinghua Shenzhen International Graduate School for assistance with grasping force measurements.

Author Contribution Statement: X.Y. designed and manufactured the actuators, conducted the experiments, analyzed data, and wrote the manuscript. X.Q. proposed the main idea, edited the manuscript and supervised the research. S.Z. reviewed, edited, and commented on the manuscript. M.Z and X.W. supervised the research and commented on the paper.

Author Disclosure Statement: The authors declare no conflict of interest.

Funding: This work was supported in part by the National High Technology Research and Development Plan of China (2015AA043505) and in part by Shenzhen Fundamental Research Funding (Grant No. JSGG20180508153002284).

References

1. Aziz S, Spinks GM. Torsional artificial muscles. **Mater. Horiz.** 2020;7:667-693.
2. Meng Q, Xiang S, Yu H. Soft Robotic Hand Exoskeleton Systems: Review and Challenges Surrounding the Technology. In: 2017 2nd International Conference on

Electrical, Automation and Mechanical Engineering (EAME 2017), Atlantis Press, 2017:186-190.
3. Martell JS, Gini G. Robotic hands: design review and proposal of new design process. **World Acad. Sci. Eng. Technol.** 2007;26:85-90.
4. Hughes J, Culha U, Giardina F, et al. Soft Manipulators and Grippers: A Review. **Front. Robot. AI.** 2016;3:69.
5. Suzuki T, Liao H, Kobayashi E, et al. Ultrasonic motor driving method for EMI-free image in MR image-guided surgical robotic system. In: 2007 IEEE/RSJ International Conference on Intelligent Robots and Systems, IEEE, 2007:522-527.
6. Li T, Li G, Liang Y, et al. Fast-moving soft electronic fish. **Sci. Adv.** 2017;3:e1602045.
7. Rus D, Tolley MT. Design, fabrication and control of soft robots. **Nature** 2015;521:467-475.
8. Foroughi J, Spinks GM, Wallace GG, et al. Torsional carbon nanotube artificial muscles. **Science** 2011;334:494-497.
9. Lima MD, Li N, De Andrade MJ, et al. Electrically, chemically, and photonically powered torsional and tensile actuation of hybrid carbon nanotube yarn muscles. **Science** 2012;338:928-932.
10. Aliev AE, Oh J, Kozlov ME, et al. Giant-stroke, superelastic carbon nanotube aerogel muscles. **Science** 2009;323:1575-1578.
11. Chun K-Y, Kim SH, Shin MK, et al. Hybrid carbon nanotube yarn artificial muscle inspired by spider dragline silk. **Nat. Commun.** 2014;5:1-9.
12. Haines CS, Lima MD, Li N, et al. Artificial muscles from fishing line and sewing thread. **Science** 2014;343:868-872.
13. Haines CS, Li N, Spinks GM, et al. New twist on artificial muscles. **Proc. Natl. Acad. Sci.** 2016;113:11709-11716.
14. Mirvakili SM, Ravandi AR, Hunter IW, et al. Simple and strong: twisted silver painted nylon artificial muscle actuated by Joule heating. In: Electroactive Polymer Actuators and Devices (EAPAD) 2014, International Society for Optics and Photonics, 2014:90560I.
15. Tobushi H, Sakuragi T, Sugimoto Y. Deformation and rotary driving characteristics of a shape-memory alloy thin strip element. **Mater. Trans.** 2008;49:151-157.
16. Gabriel K, Trimmer W, Walker J. A micro rotary actuator using shape memory alloys. **Sensors and Actuators** 1988;15:95-102.
17. Mirfakhrai T, Madden JD, Baughman RH. Polymer artificial muscles. **Mater. Today** 2007;10:30-38.
18. Kim H, Moon JH, Mun TJ, et al. Thermally responsive torsional and tensile fiber actuator based on graphene oxide. **ACS Appl. Mater.** 2018;10:32760-32764.
19. Shepherd RF, Ilievski F, Choi W, et al. Multigait soft robot. **Proc. Natl. Acad. Sci.** 2011;108:20400-20403.
20. Chou C-P, Hannaford B. Measurement and modeling of McKibben pneumatic artificial muscles. **IEEE Trans. Robot. Autom.** 1996;12:90-102.

21. Tondu B, Lopez P. Modeling and control of McKibben artificial muscle robot actuators. **IEEE Control Syst. Mag.** 2000;20:15-38.
22. Yan J, Zhang X, Xu B, et al. A new spiral-type inflatable pure torsional soft actuator. **Soft Robot.** 2018;5:527-540.
23. Sanan S, Lynn PS, Griffith ST. Pneumatic torsional actuators for inflatable robots. **J. Mech. Robot.** 2014;6:031003.
24. Fras J, Noh Y, Wurdemann H, et al. Soft fluidic rotary actuator with improved actuation properties. In: 2017 IEEE/RSJ International Conference on Intelligent Robots and Systems (IROS), IEEE, 2017:5610-5615.
25. Fang J, Yuan J, Wang M, et al. Novel accordion-inspired foldable pneumatic actuators for knee assistive devices. **Soft Robot.** 2020;7:95-108.
26. Sun Y, Song YS, Paik J. Characterization of silicone rubber based soft pneumatic actuators. In: 2013 IEEE/RSJ International Conference on Intelligent Robots and Systems, IEEE, 2013:4446-4453.
27. Khin PM, Yap HK, Ang MH, et al. Fabric-based actuator modules for building soft pneumatic structures with high payload-to-weight ratio. In: 2017 IEEE/RSJ International Conference on Intelligent Robots and Systems (IROS), IEEE, 2017:2744-2750.
28. Robertson MA, Paik J. New soft robots really suck: Vacuum-powered systems empower diverse capabilities. **Sci. Robot.** 2017;2:eaan6357.
29. Jiao Z, Zhang C, Wang W, et al. Advanced Artificial Muscle for Flexible Material-Based Reconfigurable Soft Robots. **Adv. Sci.** 2019;6:1901371.
30. Jiao Z, Ji C, Zou J, et al. Vacuum-Powered Soft Pneumatic Twisting Actuators to Empower New Capabilities for Soft Robots. **Adv. Mater. Technol.** 2019;4:1800429.
31. Mosadegh B, Polygerinos P, Keplinger C, et al. Pneumatic networks for soft robotics that actuate rapidly. **Adv. Funct. Mater.** 2014;24:2163-2170.
32. Homberg BS, Katzschmann RK, Dogar MR, et al. Haptic identification of objects using a modular soft robotic gripper. In: 2015 IEEE/RSJ International Conference on Intelligent Robots and Systems (IROS), IEEE, 2015:1698-1705.
33. Li S, Vogt DM, Rus D, et al. Fluid-driven origami-inspired artificial muscles. **Proc. Natl. Acad. Sci.** 2017;114:13132-13137.
34. Subramaniam V, Jain S, Agarwal J, et al. Design and characterization of a hybrid soft gripper with active palm pose control. **Int. J. Robot. Res.** 2020;0278364920918918.
35. Li S, Stampfli JJ, Xu HJ, et al. A vacuum-driven origami “magic-ball” soft gripper. In: 2019 International Conference on Robotics and Automation (ICRA), IEEE, 2019:7401-7408.
36. Liu X, Zhao Y, Geng D, et al. Soft Humanoid Hands with Large Grasping Force Enabled by Flexible Hybrid Pneumatic Actuators. **Soft Robot.** ahead of print. http://doi.org/10.1089/soro.2020.0001
37. Lee JA, Kim YT, Spinks GM, et al. All-solid-state carbon nanotube torsional and tensile artificial muscles. **Nano Lett.** 2014;14:2664-2669.
38. Chen P, Xu Y, He S, et al. Hierarchically arranged helical fibre actuators driven by solvents and vapours. **Nat. Nanotechnol.** 2015;10:1077-1083.

39. Mirvakili SM, Hunter IW. A torsional artificial muscle from twisted nitinol microwire. In: Electroactive Polymer Actuators and Devices (EAPAD) 2017, International Society for Optics and Photonics, 2017:101630S.
40. Mirvakili SM, Pazukha A, Sikkema W, et al. Niobium nanowire yarns and their application as artificial muscles. **Adv. Funct. Mater.** 2013;23:4311-4316.
41. Kim SH, Lima MD, Kozlov ME, et al. Harvesting temperature fluctuations as electrical energy using torsional and tensile polymer muscles. **Energy Environ. Sci.** 2015;8:3336-3344.
42. Kornbluh R, Pelrine R, Eckerle J, et al. Electrostrictive polymer artificial muscle actuators. In: Proceedings. 1998 IEEE international conference on robotics and automation (Cat. No. 98CH36146), IEEE, 1998:2147-2154.
43. Ahn CH, Wang W, Jung J, et al. Pleated film-based soft twisting actuator. **Int. J. Precis. Eng. Manuf.** 2019;20:1149-1158.
44. Pourghodrat A, Nelson CA. Disposable fluidic actuators for miniature in-vivo surgical robotics. **J. Med. Device** 2017;11:0110031–0110038.
45. Manfredi L, Putzu F, Guler S, et al. 4 DOFs hollow soft pneumatic actuator–HOSE. **Mater. Res. Express** 2019;6:045703.
46. Kline T, Kamper D, Schmit B. Control system for pneumatically controlled glove to assist in grasp activities. In: 9th International Conference on Rehabilitation Robotics (ICORR) 2005, IEEE, 2005:78-81.
47. Raparelli T, Ivanov A, Palladino FE. Textile rotary pneumatic actuator for rehabilitation. In: International conference on robotics in Alpe-Adria Danube region, Springer, 2017:727-734.
48. Sasaki D, Noritsugu T, Takaiwa M. Development of active support splint driven by pneumatic soft actuator (ASSIST). In: Proceedings of the 2005 IEEE international conference on robotics and automation, IEEE, 2005:520-525.
49. Pylatiuk C, Kargov A, Gaiser I, et al. Design of a flexible fluidic actuation system for a hybrid elbow orthosis. In: 2009 IEEE International Conference on Rehabilitation Robotics, IEEE, 2009:167-171.
50. Zhang W, Yu Z, Chen X, et al. The magneto-thermal analysis of a high torque density joint motor for humanoid robots. In: 2018 IEEE-RAS 18th International Conference on Humanoid Robots (Humanoids), IEEE, 2018:112-117.